Catalysis Science & Technology

ROYAL SOCIETY OF CHEMISTRY

COMMUNICATION

View Article Online
View Journal

Cite this: DOI: 10.1039/d6cy00362a

Received 1st April 2026,
Accepted 1st June 2026

DOI: 10.1039/d6cy00362a

rsc.li/catalysis

Ambient pressure ammonia decomposition using Ga–Co supported catalytically active liquid metal solutions

Philipp Rothgängel, [ab] Nicola Taccardi, [c] Aaron Luke Folkard, [cd] Jakob Söllner,[e] Alexander Søgaard, [c] Andreas Körner, [a] Andreas Hutzler, [a] Matthias Thommes, [e] Marco Haumann [cf] and Peter Wasserscheid *[abc]

Ga–Co supported catalytically active metal solutions (SCALMS) on silicon carbide (SiC) were successfully tested for ambient pressure ammonia decomposition in the temperature range between 480 and 580 °C. Comparison studies of a $Ga_{59}Co$ SCALMS system with their monometallic equivalents Co/SiC and Ga/SiC revealed a massively enhanced ammonia decomposition activity of the supported alloy catalyst. The $Ga_{59}Co$/SiC outperformed a monometallic benchmark Co/SiC catalyst in terms of the Co specific H_2 productivity by up to one order of magnitude. Monometallic Ga/SiC, in contrast, showed no activity for ammonia decomposition up to 580 °C. We report productivities of 487 g_{H_2} g_{Co}^{-1} h^{-1} at 5% conversion and 550 °C at a weight hourly space velocity (WHSV) of 29 000 mL_N g_{cat}^{-1} h^{-1} for our SCALMS system. Apparent activation energies ($E_{A,app}$) determined from temperature variation experiments give no indication for diffusion limitations under the applied reaction conditions. Therefore, we present a new catalyst material concept for ammonia decomposition with high potential for practical and technical application.

Introduction

In pursuit of decarbonisation, various nations have announced strategies and formed alliances focusing on hydrogen (H_2) as a renewable energy carrier, given its high gravimetric energy density (33.3 kWh kg^{-1}) and environmentally benign properties. However, large-scale storage and long-distance transportation present technical challenges due to hydrogen's low volumetric energy density (3 kWh m^3 at 20 °C and 1 bar) and small molecular size.[1–5]

Green and/or blue ammonia (NH_3) has been proposed as a promising H_2 carrier to address these limitations. Due to its high volumetric H_2 storage capacity (~108 kg_{H_2} m^3) and ease of liquefaction (*e.g.* 25 °C, 10 bar), it is a potentially cost-efficient alternative for long-distance transportation.[3,6–8] The chemically bound H_2 can be released on demand through thermal cracking, producing only nitrogen (N_2) as a byproduct, as shown in eqn (1).

$$2NH_3 \rightleftharpoons N_2 + 3H_2;\ \Delta H^0_{298} = 92.44\ \text{kJ mol}^{-1} \quad (1)$$

Using a catalyst to enhance the efficiency of hydrogen release is essential to optimise the overall net energy balance, given that the reaction requires temperatures above 500 °C due to its endothermic nature. The reaction is characterized by adsorption and desorption steps (eqn (2), (6), and (7)) and the cleavage of N–H bonds (eqn (3), (4), and (5)). N–H cleavage and the recombintaion of two adsobred nitrogen N_{ad} (eqn (7)) are the two main rate determining steps reported.[9,10] Enhanced electron transfer, electron donating additives, and structures or morpholgies allowing enhanced N recombination are ways to adress these topics. The investigation of such new, improved, and stable catalyst systems for thermal NH_3 decomposition is therefore of high interest to current research and industry.

$$NH_{3,g} + * \rightleftharpoons NH_{3,ad} \quad (2)$$

$$NH_{3,ad} + * \rightleftharpoons NH_{2,ad} + H_{ad} \quad (3)$$

$$NH_{2,ad} + * \rightleftharpoons NH_{1,ad} + H_{ad} \quad (4)$$

$$NH_{1,ad} + * \rightleftharpoons N_{ad} + H_{ad} \quad (5)$$

$$2H_{ad} \rightleftharpoons H_{2,g} + 2* \quad (6)$$

[a] *Helmholtz-Institute Erlangen-Nürnberg for Renewable Energy (IET-2), Forschungszentrum Jülich GmbH (FZJ), Cauerstraße 1, Erlangen 91058, Germany. E-mail: p.wasserscheid@fz-juelich.de*
[b] *Institute for a sustainable Hydrogen Economy (IHE), Forschungszentrum Jülich GmbH (FZJ), Brainergy Park Jülich, An der Deutschen Welle 7a, 52428, Jülich, Germany*
[c] *Lehrstuhl für Chemische Reaktionstechnik (CRT), Friedrich-Alexander-Universität Erlangen-Nürnberg (FAU), Egerlandstr. 3, Erlangen 91058, Germany. E-mail: nicola.taccardi@fau.de, peter.wasserscheid@fau.de*
[d] *School of Chemistry and Physics, University of KwaZulu-Natal, Durban, KwaZulu Natal, South Africa*
[e] *Lehrstuhl für Thermische Verfahrenstechnik (TVT), Friedrich-Alexander-Universität Erlangen-Nürnberg (FAU), Egerlandstr. 3, Erlangen 91058, Germany*
[f] *Research Centre for Synthesis and Catalysis, Department of Chemistry, University of Johannesburg, P.O. Box 524, Auckland Park 2006, South Africa*

$$2N_{ad} \rightleftharpoons N_{2,g} + 2* \quad (7)$$

Supported catalytically active liquid metal solutions (SCALMS) represent such a new class of heterogeneous catalysts. The SCALMS concept has recently attracted a lot of interest for the dehydrogenation of propane, butane, heptane, and methylcyclohexane as well as for the oligomerization of ethene.[11–20] First approaches in ammonia synthesis have also been reported.[21] Conceptually, SCALMS are composed under reaction conditions of liquid droplets of a catalytically active metal alloy on a porous support. Those alloys consist typically of a low-melting metal, such as, *e.g.*, Ga, that serves as matrix for dissolving smaller amounts of a catalytically active metal. Precious metals, like Pt, Pd or Rh, and Ni as non-precious metal have been utilized as active component of SCALMS systems so far.[11–14,20] A unique feature of SCALMS systems is that the catalytic reaction occurs at dynamically emerging single-atom active sites at the gas–liquid interface. This single-atom nature of the atomically-dispersed active metal has been demonstrated for precious metal based SCALMS systems by spectroscopic, microscopic, and theoretical studies.[11,22–24]

The scope of this study is the initial investigation of SCALMS catalysts and their general suitability for thermal NH_3 decomposition by combining commonly reported metals, such as Co, Ni, and Cu, with Ga.[14–19] A comparison between the monometallic and bimetallic supported catalysts for a selected active metal aims to provide initial insights into the feasibility and attractiveness of the SCALMS concept for ammonia cracking.

Experimental

Preparation of catalysts

For our study, we prepared the Ga–X (active metal X: Co, Ni, or Cu) on SiC materials as well as monometallic Ga on SiC and Co on SiC materials (for comparative investigations) by a combination of ultrasonication-based emulsion preparation, wet impregnation and galvanic displacement. A similar methodology had been applied by our group previously to prepare Ga–Pt and Ga–Ni SCALMS materials.[12,15,20] The galvanic replacement reaction utilizes the standard reduction potentials of Ga, Co, Ni and Cu in aqueous solution (E_{Ga^{3+}/Ga^0} = −0.53 V, E_{Co^{2+}/Co^0} = −0.28 V, E_{Ni^{2+}/Ni^0} = −0.25 V, and E_{Cu^{2+}/Cu^0} = +0.34 V) to ensure the deposition of the secondary metals (higher potential) on Ga droplets (lowest potential) as described previously.[25–30] The SiC support is expected to not participate in the reaction due to its inertness in water and its notable stability, even in the presence of HF.

The benchmark Co/SiC material was prepared using incipient wetness impregnation and calcination at 600 °C for 3 h (heating ramp 2 °C min^{-1}, dried at 150 °C for 2 h). An alternatively higher loaded Co/SiC catalyst was prepared using the same method. All details regarding the catalyst material preparation are shown in the SI.

Characterization of fresh and spent catalysts

The metal weight loadings w_{metal} and the Ga to active metal X atomic ratio (Ga_nX) have been determined using inductively coupled plasma atomic emission spectroscopy (ICP-AES). Further characterizations of the used materials were carried out using N_2 sorption, Hg porosimetry, as well as scanning electron and scanning transmission electron microscopy *via* energy-dispersive X-ray spectroscopy (SEM–EDXS and STEM–EDXS). All technical details are given in the SI.

Catalytic testing

All catalytic experiments were performed in a high-temperature set-up consisting of a tubular split furnace (Nabertherm) with one heating zone of 250 mm and an isothermal zone of 80 mm. Inert quartz tubes (*L*: 1000 mm, OD: 13 mm, ID: 9.8 mm) with three pins at a height of 555 mm from the bottom end to support the catalyst bed were used as reactors. An additional quartz capillary (*L*: 700 mm, OD: 1.6 mm, DI: 0.8 mm) containing thermocouples to determine the catalyst bed temperature was placed within the catalyst bed from the top. A total of 1.0 g of catalyst was placed on top of 0.3 g quartz wool, and 0.3 g activated carbon spheres (200 μm) to ensure a uniform gas flow. All catalysts were reduced *in situ* in a $H_2:N_2$ mixed gas flow (molar ratio of 3 : 1) at 585 °C to remove the oxide skin on the metal droplets. The reduction of gallium oxide in the presence of hydrogen and a hydrogen-activating metal has been described in several publications.[15,31–33] After this catalyst preformation procedure, the gas flow was switched to NH_3, which marks the point zero of the time on stream (TOS). The temperature was stepwise increased to 582 °C in the reactor (gray bar for the first 6 h TOS in Fig. 2). The startup behavior in each experiment was observed at a flow rate of 10 l_N h^{-1} undiluted NH_3 resulting in a weight hourly space velocity (WHSV) of 10 l_N g_{cat}^{-1} h^{-1} and at temperatures of 582 °C at atmospheric pressure. Follow-up experiments were conducted by changing temperature and gas flow. The off-gas was quantitatively analyzed in a micro gas chromatograph (Micro GC Fusion, INFICON GmbH) with two sample lines and thermal conductivity detectors (TCD), one sample line for permanent gases (carrier gas: Ar) and the other one for ammonia (carrier gas: H_2). All gases used had a purity of ≥99.999% (supplied by Air Liquide Deutschland GmbH).

Results and discussion

Catalyst characterization

Three metals, namely Co, Ni, and Cu, were selected as active metals for the Ga-based SCALMS materials tested in our ambient pressure ammonia decomposition experiments.[9,21,34–37] These SCALMS materials were prepared *via* impregnation of pre-synthesized, gallium-decorated β-SiC. Analysis of the metal content resulted in Ga loadings of 3.10–6.12 wt%, active metal loadings of 0.04–0.08 wt%, and Ga/active metal ratio values between 47 and 71 (Table 1). According to the corresponding bimetallic phase diagrams, all of these Ga-rich alloys are expected to be

Table 1 Chemical composition of the supported catalytically active liquid metal solutions (SCALMS) and monometallic catalysts prepared

	Metal loading (after calcination)/wt%		
Catalyst	Ga	Active metal	Molar ratio
$Ga_{59}Co/SiC$	3.12	0.04	59
$Ga_{47}Ni/SiC$	4.60	0.08	47
$Ga_{71}Cu/SiC$	6.12	0.08	71
Ga/SiC	4.27	—	—
Co/SiC	—	0.05	—
Co/SiC	—	1.05	—

present in the liquid state at temperatures exceeding 500 °C.[20,38–40] On β-SiC supported monometallic Ga (prepared by ultrasonication) and Co (prepared by incipient wetness impregnation) were used for comparison studies. Therefore, the metal loadings aimed to be within the same range as for the SCALMS materials (Table 1).

N_2 sorption and Hg porosimetry for the utilized SiC supports and functionalized catalysts revealed mainly meso and macro pores in accordance with supplier data (see Fig. S2 to S5 and Table S1).[41] No significant changes to the pore structure and surface areas due to the catalyst preparation methods were observed. The SCALMS materials before and after reaction were characterized using scanning electron microscopy with elemental mapping *via* energy-dispersive X-ray spectroscopy (SEM–EDXS). This method was employed to evaluate the morphology of the Ga-rich droplets on the external surface of the SiC support material and the distribution of the active metal.

Using ultrasonic emulsification, the Ga droplets were produced dispersed in isopropanol from elemental Ga and directly deposited on the substrate.[12,16] In accordance with previous works, we found after subsequent galvanic displacement using a cobalt(II) nitrate hexahydrate solution in $20_{v/v}$% water in isopropanol, that the alloy droplets were mainly located on the outer surface of the support particles.[12,16,42] Some alloy droplets were also found at the walls or in cavities larger than 10 μm. The inner pore system did not contain any observable quantities of Co–Ga (see Fig. S8). Unfortunately, the low concentrations of active metals resulted in low signal-to-noise ratios for the SEM-EDXS elemental maps. Therefore, scanning transmission electron microscopy *via* energy-dispersive X-ray spectroscopy (STEM–EDXS) with higher resolution was applied to study the Ga–Co catalysts. Fig. 1 shows images and elemental mapping for the $Ga_{59}Co/SiC$ SCALMS as-prepared and after use in catalysis. In both samples the Ga-droplets were always associated with Co-signals. This was expected due to the galvanic displacement of Co on the Ga droplets during preparation. After use in catalysis, the formation of a Co-rich cluster of about 45 nm was observed within the Ga droplet. This may indicate some redistribution of the bimetallic phase and phase separation within the droplet. This may have occurred during the cool-down of the reactor at the end of the experiment. Further microscopic images (including monometallic Co/SiC) are found in the SI (Fig. S6 and S7). This phenomenon has been reported on multiple occasions in the context of liquid metal systems following cooling and subsequent resolidification. Zuraiqi *et al.* observed a Cu-rich Cu–Ga intermetallic particle that was embedded in a Ga droplet. Upon heating the sample to the reaction temperature, complete dissolution of the Cu–Ga particle in Ga was observed.[43] In their studies on Ga–Ni and Ga–Pt SCALMS systems, Søgaard *et al.* and Madubuko *et al.*, respectively, demonstrated the existence of intermetallic species by means of spectroscopy and DFT simulations, that dissolve completely or partially in the surrounding liquid Ga matrix. The presence of single metal atoms has been observed and predicted to appear at the surface of the

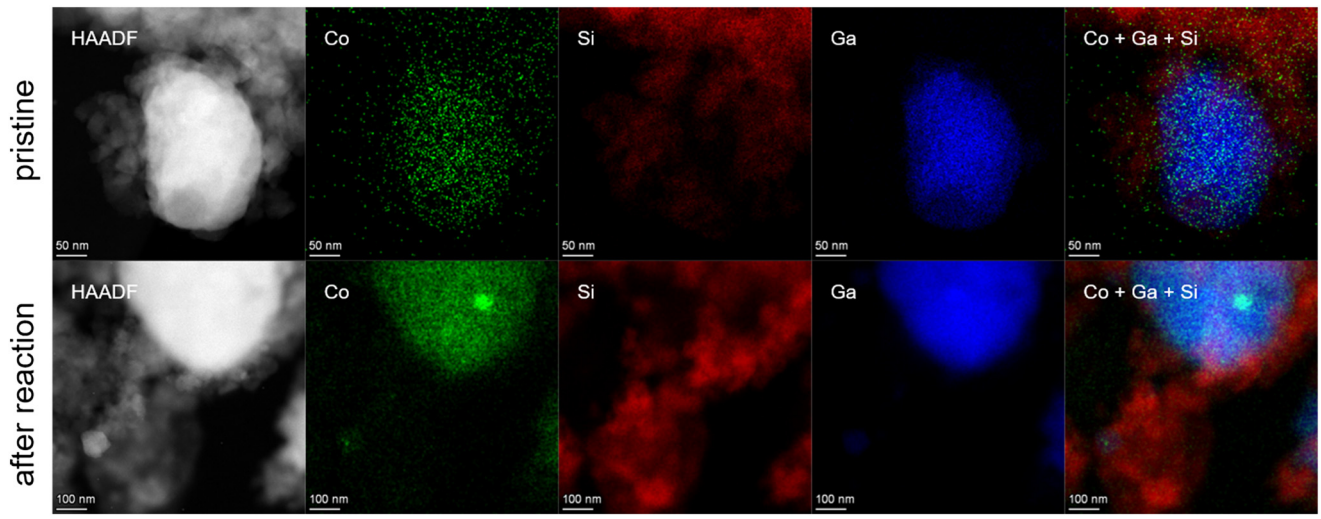

Fig. 1 STEM–EDX images of a $Ga_{59}Co/SiC$ catalyst before (as-prepared) and after use in the ammonia decomposition reaction. The images show that Co signals are associated with Ga; after use in NH_3 decomposition, the formation of a Co cluster is observed.

liquid metal droplets, while potential solid or amorphous intermetallics submerge in the bulk.[29,44] It is reasonable to hypothesize that the Ga-Co system behaves in a similar way.

Characterization of the Co-containing samples by XRD revealed in the as-prepared and used state no evidence for the formation of solid intermetallic Ga–Co species. It should be noted that the Co signals were in general low even for high Co loadings so that low signal-to-noise ratios were found in most samples (see Fig. S9 for more details).

Catalytic screening

The performance of the three SCALMS systems in NH_3 decomposition was evaluated at 582 °C and under atmospheric pressure in a quartz tube fixed-bed reactor using an undiluted NH_3 feed stream. The blank quartz tube reactor and monometallic Ga/SiC displayed negligible conversion levels in the respective blank experiments (see Fig. S10). Of the three metals studied, the presence of Co within the liquid Ga matrix (*i.e.*, the $Ga_{59}Co$/SiC SCALMS catalyst) resulted in the highest conversion of NH_3 (Fig. 2A). No activity was observed for $Ga_{71}Cu$/SiC SCALMS, while the $Ga_{47}Ni$/SiC SCALMS showed conversions below 5.0%. The Ga–Co SCALMS system showed an activation period of 13 h TOS and reached at this time a conversion level of 15.9 ± 0.1%, followed by slow deactivation to reach a conversion of 12.1 ± 0.1% after 54 h TOS. For the Ga–Ni SCALMS system under investigation the initial activation period was around 10 h TOS, after which the system reached an ammonia conversion of 4.2 ± <0.1% followed also by slow deactivation. The Ga–Ni system reached 2.9 ± <0.1% after 54 h TOS. The observed initial activation phase can be explained by the reduction of a thin, passivating GaO_x skin on the alloy droplets that remains even after H_2 pretreatment, as previously described by our group.[20,29] The passivating skin is further reduced by activated hydrogen during the ammonia decomposition induced by active species, such as Co and Ni.[12,20,30] We hypothesize that the deactivation of the SCALMS systems is mainly caused by trace water impurities within the supplied ammonia ($H_2O \leq 5$ vol. ppm), that accumulated on the SCALMS system.[12,45,46] Fig. S12 in the SI shows an extended TOS (>330 h) experiment for a $Ga_{59}Co$ SCALMS, indicating that the system reached a steady-state after the initial deactivation phase. Furthermore, it was observed that water was expelled from the system during the repetitive flushing process with H_2/N_2 mixtures, H_2, N_2 or Ar.

Based on these screening results, we focused our further investigations on the $Ga_{59}Co$ SCALMS system. To elucidate the promoting effect of dissolving Co into liquid Ga, we studied a monometallic Co/SiC catalyst (0.05 wt% Co) prepared by incipient wetness impregnation under identical conditions. The catalytic results are also shown in Fig. 2. Like the Ga–Co SCALMS, the Co/SiC catalyst shows an activation phase in the first 13 h TOS followed by a flattened further increase in ammonia conversion. The conversion increased from 3.2 ± <0.1% after 13 h TOS to 4.1 ± <0.1% after 54 h TOS. Remarkably, also after 54 h TOS, the ammonia conversion of the monometallic Co/SiC catalyst was about three times lower than that if the $Ga_{59}Co$ SCALMS system after 54 h TOS and about four times lower comparing the maximum conversions of both catalyst systems. This impressively supports our hypothesis that the special SCALMS nature of $Ga_{59}Co$ SCALMS leads to a very significant activity boost in ammonia decomposition.

Fig. 2B shows the specific H_2 productivities per mass of active metal. These values allow us to compare the level of metal utilization and the specific activity of each active metal in NH_3 decomposition. Herein, the $Ga_{59}Co$ SCALMS system

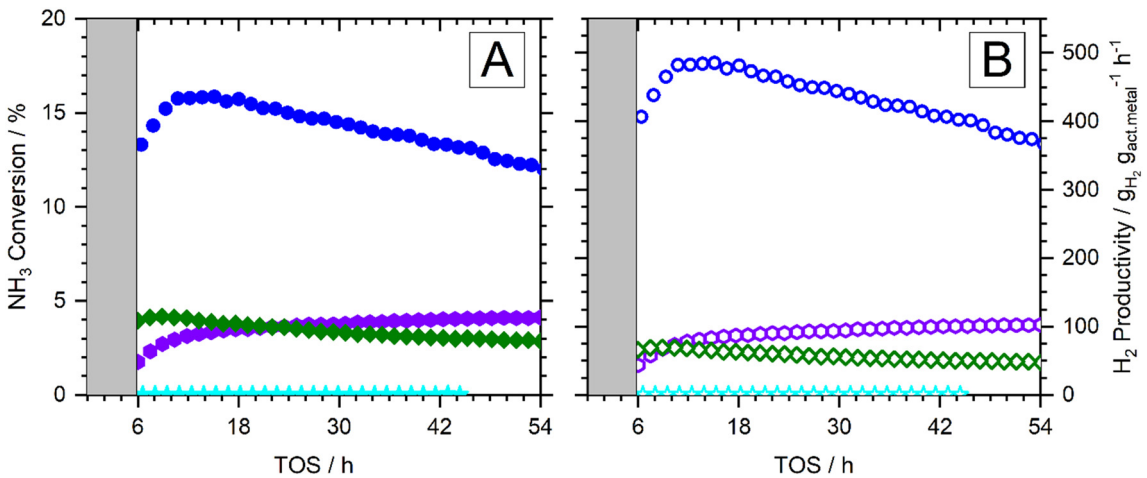

Fig. 2 NH_3 conversion (Fig. 2A, filled symbols) and H_2 productivity specific to the active metal mass (Fig. 2B, hollow symbols) over 54 h time on stream (TOS) for four different ammonia decomposition catalysts at equal reaction conditions: SCALMS $Ga_{59}Co$/SiC (blue circle ●, m_{cat} = 1.00 g, V_{cat} = 1.8 ml, w_{Co} = 0.04 wt%, w_{Ga} = 3.12 wt%); $Ga_{47}Ni$/SiC (green diamond ◆, m_{cat} = 1.00 g, V_{cat} = 1.5 ml, w_{Ni} = 0.04 wt%, w_{Ga} = 3.12 wt%); $Ga_{71}Cu$/SiC (cyan star ★, m_{cat} = 1.00 g, V_{cat} = 1.9 ml, w_{Cu} = 0.08 wt%, w_{Ga} = 6.12 wt%), and monometallic Co/SiC (purple hexagon ⬢, m_{cat} = 1.00 g, V_{cat} = 1.5 ml, w_{Co} = 0.05 wt%). Reaction conditions: T_{cat} = 582 °C, p_{total} = 1 bar(a), WHSV = 10 l_N g_{cat}^{-1} h^{-1}. The figures show every 36th data point for clarity.

shows a metal specific activity of 486 $g_{H_2}\ g_{Co}^{-1}\ h^{-1}$, which is close to seven times higher than the 70 $g_{H_2}\ g_{Ni}^{-1}\ h^{-1}$ found for the Ga–Ni system. The monometallic Co on SiC showed productivities up to 103 $g_{H_2}\ g_{Co}^{-1}\ h^{-1}$.

Influence of SCALMS on cobalt activity

In a next set of experiments, we studied the hydrogen productivity in ammonia cracking as a function of temperature comparing the $Ga_{59}Co$ SCALMS system and the monometallic Co/SiC catalyst. These experiments were carried out in the temperature range between 485 and 550 °C for $Ga_{59}Co$ SCALMS and between 550 and 582 °C for Co/SiC, respectively. Note, that these experiments were carried out at varying NH_3 flow rates between 30 and 450 $ml_N\ min^{-1}$ in order to adjust an equal conversion level of 5 ± 0.5% independent on the applied reaction temperature. The resulting Co-specific H_2 productivities as a function of catalyst bed temperatures are shown in Fig. 3.

Apart from the much higher Co-specific hydrogen productivity for the SCALMS system, these experiments revealed a significantly stronger temperature dependency of $Ga_{59}Co$/SiC SCALMS compared to the Co/SiC catalyst. Ga_{59}-Co/SiC SCALMS showed an exponential productivity increase from 30 $g_{H_2}\ g_{Co}^{-1}\ h^{-1}$ at 486 °C up to 487 $g_{H_2}\ g_{Co}^{-1}\ h^{-1}$ at 548 °C. In sharp contrast, for Co/SiC the Co-based specific productivity was only 35 $g_{H_2}\ g_{Co}^{-1}\ h^{-1}$ at 550 °C and increased up to 111 $g_{H_2}\ g_{Co}^{-1}\ h^{-1}$ at 582 °C. Remarkably, the SCALMS productivity outperformed the monometallic Co/SiC by a factor of 14 at a temperature of 550 °C. We hypothesize that this drastic increase in activity is related to the single-atom nature of Co at the catalytic interface of the SCALMS system and due to the high mobility of the supported liquid alloy at this elevated temperature.[22–24] The mobility of these Co single atoms may help to recombine adsorbed nitrogen atoms to form N_2 which is the commonly reported rate determining steps in ammonia decomposition for metals like Co and Ni.[9,10,47] Additionally, there is a possibility of a spillover of nitrogen to Ga, accompanied by the formation of dynamic Ga–N species, as reported by Zuraiqi *et al.* during ammonia synthesis utilizing liquid metal Ga–Cu.[21] Analogous effects for Ga–Rh SCALMS in the activation of propane during propane dehydrogenation have been reported by our group.[11] Furthermore, the specific electronic nature of Co surrounded by Ga atoms at the liquid metal interface is expected to further promote nitrogen recombination by an electron donation effect.[11,43,48–52]

Fig. 4 shows the Arrhenius plots using the natural logarithm of the H_2 productivities for both catalysts. Equal conversion rates were used to avoid influences of different product partial pressures and of different distances from equilibrium conversion. The slope of the plotted data was used to calculate the apparent activation energies ($E_{A,app}$) for both systems. They were determined to be 226 ± 6 kJ mol^{-1} for $Ga_{59}Co$/SiC SCALMS and 215 ± 9 kJ mol^{-1} for the monometallic Co/SiC, respectively. From these data, we conclude that both reactions take place in the kinetic regime.[53] This is no surprise given the meso- and microporous nature of the applied SiC support and the fact that our SCALMS preparation by ultrasonication leads to support decoration with alloy droplets mainly on the outer surface (see SI for the respective microscopic results, Fig. S8).[12,16,41,42] Film diffusion limitation can be safely excluded from the $E_{A,app}$ values determined.[53]

Co-catalyzed ammonia decomposition is reported to be a structure sensitive reaction. Supported Co particle in the size range of 10 to 20 nm have been shown to exhibit the highest

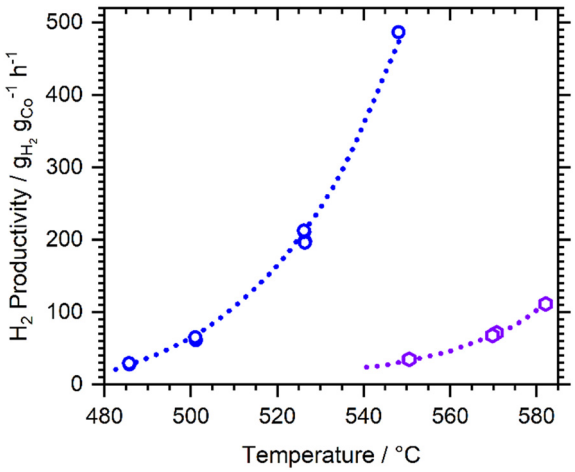

Fig. 3 H_2 productivity specific to the Co mass at 5 ± 0.5% NH_3 conversion at different catalyst temperatures for $Ga_{59}Co$/SiC (blue circle ○, m_{cat} = 1.00 g, V_{cat} = 1.8 ml, w_{Co} = 0.04 wt%, w_{Ga} = 3.12 wt%, WHSV = 2–29 $l_N\ g_{cat}^{-1}\ h^{-1}$, p_{total} = 1 bar(a)) and Co/SiC (purple hexagon ⬡, m_{cat} = 1.00 g, V_{cat} = 1.5 ml, w_{Co} = 0.05 wt%, WHSV = 3–9 $l_N\ g_{cat}^{-1}\ h^{-1}$, p_{total} = 1 bar(a)). Dotted lines to guide the eye.

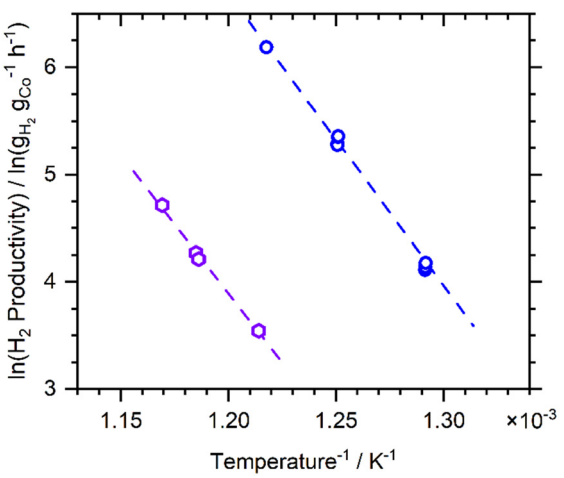

Fig. 4 Arrhenius plot using the natural logarithm of the Co mass-specific H_2 productivity at 5 ± 0.5% NH_3 conversion plotted over the inverse catalyst temperature for $Ga_{59}Co$/SiC (blue circle ○, m_{cat} = 1.00 g, V_{cat} = 1.8 ml, w_{Co} = 0.04 wt%, w_{Ga} = 3.12 wt%, WHSV = 4–29 $l_N\ g_{cat}^{-1}\ h^{-1}$, p_{total} = 1 bar(a)) and Co/SiC (purple hexagon ⬡, m_{cat} = 1.00 g, V_{cat} = 1.5 ml, w_{Co} = 0.05 wt%, WHSV = 3–9 $l_N\ g_{cat}^{-1}\ h^{-1}$, p_{total} = 1 bar(a). Dashed lines indicate linear fits.

Table 2 Co mass-based hydrogen productivity through ammonia decomposition of various SiC supported Co-based catalyst – comparison of data from this work with literature data obtained under comparable conditions

Catalyst	Co loading/wt%	WHSV/ml_{N,NH_3} g_{cat}^{-1} h^{-1}	Temperature/°C	NH_3 conversion/%	H_2 productivity/g_{H_2} g_{Co}^{-1} h^{-1}	Ref.
$Ga_{59}Co/SiC$	0.04	29 000	550	5.1	487	This work
Co/SiC	0.05	3000	550	4.6	34	This work
Co/SiC	1.05	91 200	550	4.6	54	This work
Co/SiC	10	30 000	550	43.8[a]	18[b]	61
Co/SiC	25	30 000	550	73.2	12[b]	61
Co/SiC	35	30 000	550	78.3	12[b]	62
Co/SiO_2	10	30 000	550	70	28	57, 63
5CoNa/Ti-NT	3.5	6000	550	23	5	56
Co/CNTs	5.0	36 000	550	—	29[b]	64
$Ga_{59}Co/SiC$	0.04	4500	500	4.8	65	This work
Co/SiC	1.05	18 700	515	4.7	12	This work
Co/SiO_2	10	30 000	500	42.2	17	63
Co/BaNH	4.8	36 000	500	—	50[b]	64
Co/CNTs	5.0	36 000	500	—	13[b]	64
Co/CNTs	4.1	5000	500	8	1.5	57, 65
Co in Al_2O_3 matrix	95	18 000	500	72	9	52, 66

Experiments at atmospheric pressure and pure ammonia flow (no gas dilution). [a] Determined from graphs using the open source software ImageJ.[67] [b] Calculated from published and determined data.

activities.[37,52,54–57] Therefore, we prepared a Co catalyst on SiC with a 21 times higher Co loading (1.05 wt%) leading to particle sizes of about 10 nm as confirmed by STEM–EDX images (see Fig. S6). The experiments with this higher loaded and ideally sized Co/SiC catalyst showed indeed 1.6 higher activity (comparison at 550 °C), but still the SCALMS catalyst remains 9 times more active than this optimized Co/SiC material (see Fig. S11). Table 2 compares the hydrogen productivities obtained in this study to other reported Co-based ammonia decomposition catalysts from the literature. Such comparison is challenging, as also addressed by Ristig *et al.*,[9] because of the variability of conditions and conversion levels as well as sometimes lack of detailed experimental information in the ammonia decomposition literature. Despite these difficulties, it is fair to state that the hydrogen productivity of our $Ga_{59}Co/SiC$ SCALMS catalyst exceeds all reported example of Co-based ammonia decomposition catalysts at 500 and 550 °C by far. Note that the productivity of our monometallic Co/SiC catalyst is well in line with other monometallic Co systems described in the literature and shown in Table 2. This underscores the considerable potential of SCALMS-type catalysts for the further development of ammonia decomposition towards productivity levels that were previously unattainable for base metals and reserved for the use of precious metals, such as Ru-based catalysts.[9,58–60]

Conclusion

In summary, we have demonstrated in this work the substantial potential of Ga–Co SCALMS materials as heterogeneous catalysts for the decomposition of ammonia under technical relevant conditions. The SCALMS concept appears to be highly beneficial for specific requirements of ammonia decomposition: i) it offers a very efficient use of Co due to the single atom nature of Co in Ga-based SCALMS; ii) the Ga surrounding of Co seem to alter the electronic properties of Co in a beneficial way for ammonia decomposition; iii) the highly dynamic liquid alloy nature seem to promote the recombination of adsorbed nitrogen atoms to form N_2. These beneficial effects and their combination open new avenues for the further optimization of ammonia decomposition catalysis, avenues that go clearly beyond traditional structure-sensitive surface catalysis and avoid the use of precious metals.

Author contributions

Philipp Rothgängel: resources, investigation, formal analysis, validation, visualization, writing – original draft preparation and data curation. Nicola Taccardi: resources and methodology (SCALMS catalysts), writing – review & editing. Aaron Luke Folkard: resources and methodology. Jakob Söllner: investigation, formal analysis and visualization. Alexander Søgaard: resources. Andreas Körner: investigation and visualization. Andreas Hutzler: supervision and investigation. Matthias Thommes: supervision and funding acquisition. Marco Haumann: writing – review & editing, conceptualization, supervision, project administration, funding acquisition. Peter Wasserscheid: writing – review & editing, conceptualization, supervision, project administration, funding acquisition. All authors have given approval to the final version of the manuscript.

Conflicts of interest

There are no conflicts to declare.

Data availability

Data for this article, including figures and plot data are available at Zenodo at https://doi.org/10.5281/zenodo.14968866.

The data supporting this article have been included as part of the supplementary information (SI).

Supplementary information is available. See DOI: https://doi.org/10.1039/d6cy00362a.

Acknowledgements

PRo, NTa, MHa, and PWa thank for financial support by the European Research Council through Project 786475: Engineering of Supported Catalytically Active Liquid Metal Solutions. Additional infrastructural and financial support by the German Research Foundation (DFG) through the Collaborative research centers CRC 1452 is gratefully acknowledged.

References

1 M. Heeg, *China erklärt Wasserstoff zur Zukunftstechnologie*, Vulkan-Verlag GmbH, 2025.
2 M. Genovese, A. Schlüter and E. Scionti, *et al.*, Power-to-hydrogen and hydrogen-to-X energy systems for the industry of the future in Europe, *Int. J. Hydrogen Energy*, 2023, **48**, 16545–16568.
3 *African Green Hydrogen Report 2025: Potential to Power: Advancing Green Hydrogen Across Africa*, Deutsche Gesellschaft für Internationale Zusammenarbeit (GIZ) GmbH, 2025.
4 Green Hydrogen Organisation, The Africa Green Hydrogen Alliance (AGHA), https://gh2.org/agha, (2026, accessed 23 February 2026).
5 S. Peters, A. M. Abdel-Mageed and S. Wohlrab, Thermocatalytic Ammonia Decomposition – Status and Current Research Demands for a Carbon-Free Hydrogen Fuel Technology, *ChemCatChem*, 2023, **15**, e202201185.
6 H. Mashhadimoslem, M. Safarzadeh Khosrowshahi and M. Delpisheh, *et al.*, Green ammonia to Hydrogen: Reduction and oxidation catalytic processes, *Chem. Eng. J.*, 2023, **474**, 145661.
7 C. Zink, *Kenya PtX Atlas shows potential for green ammonia from renewable energies*, 2025.
8 R. Suda, *Japan looks to US, Australia for ammonia supply chain*, Argus Media Group, 2021.
9 S. Ristig, M. Poschmann and J. Folke, *et al.*, Ammonia Decomposition in the Process Chain for a Renewable Hydrogen Supply, *Chem. Ing. Tech.*, 2022, **94**, 1413–1425, DOI: 10.1002/cite.202200003.
10 J. C. Ganley, F. S. Thomas and E. G. Seebauer, *et al.*, A Priori Catalytic Activity Correlations: The Difficult Case of Hydrogen Production from Ammonia, *Catal. Lett.*, 2004, **96**, 117–122, DOI: 10.1023/B:CATL.0000030108.50691.d4.
11 N. Raman, S. Maisel and M. Grabau, *et al.*, Highly Effective Propane Dehydrogenation Using Ga-Rh Supported Catalytically Active Liquid Metal Solutions, *ACS Catal.*, 2019, **9**, 9499–9507.
12 M. Wolf, A. L. de Oliveira and N. Taccardi, *et al.*, Dry reforming of methane over gallium-based supported catalytically active liquid metal solutions, *Commun Chem*, 2023, **6**, 1–11, https://www.nature.com/articles/s42004-023-01018-w.
13 N. Taccardi, M. Grabau and J. Debuschewitz, *et al.*, Gallium-rich Pd–Ga phases as supported liquid metal catalysts, *Nature Chem*, 2017, **9**, 862–867, https://www.nature.com/articles/nchem.2822.
14 O. Sebastian, S. Nair and N. Taccardi, *et al.*, Stable and Selective Dehydrogenation of Methylcyclohexane using Supported Catalytically Active Liquid Metal Solutions – Ga 52 Pt/SiO 2 SCALMS, *ChemCatChem*, 2020, **12**, 4533–4537.
15 O. Sebastian, A. Al-Shaibani and N. Taccardi, *et al.*, Ga-Pt supported catalytically active liquid metal solutions (SCALMS) prepared by ultrasonication – influence of synthesis conditions on n-heptane dehydrogenation performance, *Catal. Sci. Technol.*, 2023, **13**, 4435–4450.
16 N. Raman, M. Wolf and M. Heller, *et al.*, GaPt Supported Catalytically Active Liquid Metal Solution Catalysis for Propane Dehydrogenation-Support Influence and Coking Studies, *ACS Catal.*, 2021, **11**, 13423–13433.
17 M. Wolf, N. Raman and N. Taccardi, *et al.*, Coke Formation during Propane Dehydrogenation over Ga-Rh Supported Catalytically Active Liquid Metal Solutions, *ChemCatChem*, 2020, **12**, 1085–1094.
18 M. Wolf, N. Raman and N. Taccardi, *et al.*, Capturing spatially resolved kinetic data and coking of Ga-Pt supported catalytically active liquid metal solutions during propane dehydrogenation in situ, *Faraday Discuss.*, 2021, **229**, 359–377.
19 T. Zimmermann, N. Madubuko and P. Groppe, *et al.*, Supraparticles on beads for supported catalytically active liquid metal solutions – the SCALMS suprabead concept, *Mater. Horiz.*, 2023, **10**, 4960–4967.
20 A. Søgaard, A. L. de Oliveira and N. Taccardi, *et al.*, Ga-Ni supported catalytically active liquid metal solutions (SCALMS) for selective ethylene oligomerization, *Catal. Sci. Technol.*, 2021, **11**, 7535–7539.
21 K. Zuraiqi, Y. Jin and C. J. Parker, *et al.*, Unveiling metal mobility in a liquid Cu–Ga catalyst for ammonia synthesis, *Nat. Catal.*, 2024, **7**, 1044–1052.
22 T. Bauer, S. Maisel and D. Blaumeiser, *et al.*, Operando DRIFTS and DFT Study of Propane Dehydrogenation over Solid- and Liquid-Supported Ga x Pt y Catalysts, *ACS Catal.*, 2019, **9**, 2842–2853.
23 M. Kettner, S. Maisel and C. Stumm, *et al.*, Pd-Ga model SCALMS: Characterization and stability of Pd single atom sites, *J. Catal.*, 2019, **369**, 33–46, https://www.sciencedirect.com/science/article/pii/S0021951718304111.
24 S. Maisel, *Investigation of Novel Liquid Metal Catalysts with Density-Functional Methods*, Friedrich-Alexander-Universität Erlangen-Nürnberg (FAU), Erlangen, 2021.
25 C. E. Housecroft and A. G. Sharpe, *Inorganic chemistry*, Pearson, Harlow, England, Munich, 4th edn, 2012.
26 L. Castilla-Amorós, D. Stoian and J. R. Pankhurst, *et al.*, Exploring the Chemical Reactivity of Gallium Liquid Metal

Nanoparticles in Galvanic Replacement, *J. Am. Chem. Soc.*, 2020, **142**, 19283–19290.
27 A. J. Bard, R. Parsons and J. Jordan, *Standard Potentials in Aqueous Solution*, Routledge, 1st edn, 2017.
28 Representative Standard Reduction Potentials at 298 K, in *Coordination Chemistry*, ed. T. Tanase and Y. Ishii, Royal Society of Chemistry, 2024, pp. 426–430.
29 N. Madubuko, T.-E. Hsieh and N. Vorlaufer, *et al.*, Reductive Treatment of Ga–Pt-Supported Catalytically Active Liquid Metal Solutions (SCALMS) for Propane Dehydrogenation, *ACS Catal.*, 2025, **15**, 12436–12449.
30 A. Søgaard, *Ga-Ni Supported Catalytically Active Liquid Metal Solutions (SCALMS) for Selective Alkene Oligomerisation*, 2024.
31 M. J. Regan, H. Tostmann and P. S. Pershan, *et al.*, X-ray study of the oxidation of liquid-gallium surfaces, *Phys. Rev. B: Condens. Matter Mater. Phys.*, 1997, **55**, 10786–10790.
32 M. D. Dickey, R. C. Chiechi and R. J. Larsen, *et al.*, Eutectic Gallium-Indium (EGaIn): A Liquid Metal Alloy for the Formation of Stable Structures in Microchannels at Room Temperature, *Adv Funct Materials*, 2008, **18**, 1097–1104.
33 L. Rodríguez, D. Romero and D. Rodríguez, *et al.*, Dehydrogenation of n-butane over Pd–Ga/Al2O3 catalysts, *Appl. Catal., A*, 2010, **373**, 66–70, https://www.sciencedirect.com/science/article/pii/S0926860X09007492.
34 R. E. Yakovenko, T. V. Krasnyakova and A. N. Saliev, *et al.*, Ammonia Decomposition over Cobalt-Based Silica-Supported Fischer-Tropsch Synthesis Catalysts, *Kinet. Catal.*, 2023, **64**, 180–190, DOI: 10.1134/s002315842302009x.
35 K. E. Lamb, M. D. Dolan and D. F. Kennedy, Ammonia for hydrogen storage; A review of catalytic ammonia decomposition and hydrogen separation and purification, *Int. J. Hydrogen Energy*, 2019, **44**, 3580–3593, https://www.sciencedirect.com/science/article/pii/S0360319918339272.
36 Z. Lendzion-Bielun, U. Narkiewicz and W. Arabczyk, Cobalt-based Catalysts for Ammonia Decomposition, *Materials*, 2013, **6**, 2400–2409.
37 I. Lucentini, X. Garcia and X. Vendrell, *et al.*, Review of the Decomposition of Ammonia to Generate Hydrogen, *Ind. Eng. Chem. Res.*, 2021, **60**, 18560–18611.
38 H. Okamoto, Co-Ga (Cobalt-Gallium), *J Phs Eqil and Diff*, 2005, **26**, 197.
39 H. Okamoto, Ga-Ni (Gallium-Nickel), *J Phs Eqil and Diff*, 2010, **31**, 575–576.
40 P. Villars and H. Okamoto, Cu–Ga Binary Phase Diagram 0–100 at% Ga: Datasheet from "PAULING FILE Multinaries Edition – 2022" in SpringerMaterials (https://materials.springer.com/isp/phase-diagram/docs/c_0104092), Springer-Verlag Berlin Heidelberg & Material Phases Data System (MPDS), Switzerland & National Institute for Materials Science (NIMS), Japan, https://materials.springer.com/isp/phase-diagram/docs/c_0104092.
41 *SiC product Presentation*, SICAT Catalysts Inc., 2017.
42 N. Raman, J. Söllner and N. Madubuko, *et al.*, Top-down vs. bottom-up synthesis of Ga–based supported catalytically active liquid metal solutions (SCALMS) for the dehydrogenation of isobutane, *Chem. Eng. J.*, 2023, **475**, 146081.
43 K. Zuraiqi, A. Zavabeti and F.-M. Allioux, *et al.*, Liquid Metals in Catalysis for Energy Applications, *Joule*, 2020, **4**, 2290–2321.
44 A. Søgaard, T.-E. Hsieh and J. Steffen, *et al.*, Single Atom Sites in Ga-Ni Supported Catalytically Active Liquid Metal Solutions (SCALMS) for Selective Ethylene Oligomerization, *ChemPhysChem*, 2025, **26**, e202400651.
45 M. Wolf, N. Fischer and M. Claeys, Water-induced deactivation of cobalt-based Fischer–Tropsch catalysts, *Nat. Catal.*, 2020, **3**, 962–965.
46 AMMONIAK N50 | Air Liquide, https://de.airliquide.com/catalogue/ammoniak-n50/P0914?srsltid=AfmBOoqyCp7ktLCgmKquCJ0d8ilTD06h9ZJM6PsT5EqXpVD3YWZ17zke, (2026, accessed 11 May 2026).
47 S. Chen, J. Jelic and D. Rein, *et al.*, Highly loaded bimetallic iron-cobalt catalysts for hydrogen release from ammonia, *Nat. Commun.*, 2024, **15**, 871.
48 L. Su, F. Zeng and J. Wang, *et al.*, Boosting ammonia decomposition for hydrogen production over Co/CeO 2 catalysts via Sr doping, *Catal. Sci. Technol.*, 2026, **16**, 2394–2404.
49 N. P. Maqunga, N. Opembe and M. Mathaba, *et al.*, Advances in catalysts development and catalytic activity trends of conventional metal oxides and inorganic perovskites for hydrogen production via ammonia decomposition: a review, *Discov Catal*, 2026, **3**, 5.
50 H. Zhang, Y. A. Alhamed and A. Al-Zahrani, *et al.*, Tuning catalytic performances of cobalt catalysts for clean hydrogen generation via variation of the type of carbon support and catalyst post-treatment temperature, *Int. J. Hydrogen Energy*, 2014, **39**, 17573–17582.
51 M. Moritz, S. Maisel and N. Raman, *et al.*, Supported Catalytically Active Liquid Metal Solutions: Liquid Metal Catalysis with Ternary Alloys, Enhancing Activity in Propane Dehydrogenation, *ACS Catal.*, 2024, **14**, 6440–6450.
52 T. E. Bell and L. Torrente-Murciano, H2 Production via Ammonia Decomposition Using Non-Noble Metal Catalysts: A Review, *Top. Catal.*, 2016, **59**, 1438–1457.
53 A. Jess and P. Wasserscheid, *Chemical technology: From principles to products*, Wiley-VCH, Weinheim, 2nd edn, 2020.
54 S. Podila, Y. A. Alhamed and A. A. AlZahrani, *et al.*, Hydrogen production by ammonia decomposition using Co catalyst supported on Mg mixed oxide systems, *Int. J. Hydrogen Energy*, 2015, **40**, 15411–15422.
55 Y.-Q. Gu, Z. Jin and H. Zhang, *et al.*, Transition metal nanoparticles dispersed in an alumina matrix as active and stable catalysts for CO x -free hydrogen production from ammonia, *J. Mater. Chem. A*, 2015, **3**, 17172–17180.
56 H. A. Lara-García, J. A. Mendoza-Nieto and H. Pfeiffer, *et al.*, COx-free hydrogen production from ammonia on novel cobalt catalysts supported on 1D titanate nanotubes, *Int. J. Hydrogen Energy*, 2019, **44**, 30062–30074.
57 S. Kim, Y. W. Kim and I. Chung, *et al.*, Recent Advances and Strategies for Co-Based Catalysts in Ammonia Decomposition for Hydrogen Production, *Adv Energy and Sustain Res*, 2025, **6**, 2400406.

58 M. Pinzón, C. Martín and A. Romero, *et al.*, Efficient hydrogen production from ammonia over Ru-Co/SiC catalysts, *Catal. Today*, 2025, **458**, 115378.
59 M. Pinzón, A. Romero and A. de Lucas Consuegra, *et al.*, Hydrogen production by ammonia decomposition over ruthenium supported on SiC catalyst, *J. Ind. Eng. Chem.*, 2021, **94**, 326–335.
60 S.-F. Yin, B.-Q. Xu and C.-F. Ng, *et al.*, Nano Ru/CNTs: a highly active and stable catalyst for the generation of CO-free hydrogen in ammonia decomposition, *Appl. Catal., B*, 2004, **48**, 237–241.
61 G. Li, Y. Tan and Z. Lei, *et al.*, Preparation of high surface area carborundum-supported cobalt catalysts for hydrogen production by ammonia decomposition, *Carbon Lett.*, 2023, **33**, 899–908, https://link.springer.com/article/10.1007/s42823-023-00471-w.
62 R. Xu, F. Yin and J. Zhang, *et al.*, Preparation of Co/SiC catalyst and its catalytic activity for ammonia decomposition to produce hydrogen, *Catal. Today*, 2024, **437**, 114774.
63 Z.-W. Wu, X. Li and Y.-H. Qin, *et al.*, Ammonia decomposition over SiO2-supported Ni–Co bimetallic catalyst for COx-free hydrogen generation, *Int. J. Hydrogen Energy*, 2020, **45**, 15263–15269.
64 P. Yu, H. Wu and J. Guo, *et al.*, Effect of BaNH, CaNH, Mg3N2 on the activity of Co in NH3 decomposition catalysis, *J. Energy Chem.*, 2020, **46**, 16–21.
65 J. Zhang, M. Comotti and F. Schüth, *et al.*, Commercial Fe- or Co-containing carbon nanotubes as catalysts for NH3 decomposition, *Chem. Commun.*, 2007, 1916–1918.
66 Z.-S. Zhang, X.-P. Fu and W.-W. Wang, *et al.*, Promoted porous Co3O4-Al2O3 catalysts for ammonia decomposition, *Sci. China Chem.*, 2018, **61**, 1389–1398.
67 C. A. Schneider, W. S. Rasband and K. W. Eliceiri, NIH Image to ImageJ: 25 years of image analysis, *Nat. Methods*, 2012, **9**, 671–675.